A EUROPEAN JOURNAL

CHEMPHYSCHEM

OF CHEMICAL PHYSICS AND PHYSICAL CHEMISTRY

Accepted Article

Title: FRET based solid state luminescent sensor for glyphosate using calixarene grafted ruthenium(II) bipyridine doped silica nanoparticle

Authors: Bosco Christin Maria Arputham Ashwin, Chokalingam Saravanan, Thambusamy Stalin, Paulpandian Muthu Mareeswaran, and Seenivasan Rajagopal

To be cited as: *ChemPhysChem* 10.1002/cphc.201800447

Link to VoR: http://dx.doi.org/10.1002/cphc.201800447

A Journal of ChemPubSoc Europe

WILEY-VCH www.chemphyschem.org

ARTICLE WILEY-VCH

FRET based solid state luminescent sensor for glyphosate using calixarene grafted ruthenium(II)bipyridine doped silica nanoparticle

Bosco Christin Maria Arputham Ashwin,[a] Chokalingam Saravanan,[a] Thambusamy Stalin,[a] Paulpandian Muthu Mareeswaran*[a] and Seenivasan Rajagopal*[b]

Abstract: A calixarene functionalized luminescent nanoparticle was successfully fabricated for the FRET based selective and sensitive detection of organophosphorus pesticide, Glyphosate (GP). The *p*-tert-butylcalix[4]arene was grafted over the surface of $[Ru(bpy)_3]^{2+}$ incorporated SiNps to produce self-assembled nanosensors (RSC). The FRET was switched on in the presence of GP by means of energy transfer due to the binding with *p*-tert-butylcalix[4]arene grafted on the surface of RSC. The FRET efficiency of GP-RSC system was increased gradually with the addition of GP. The FRET efficiency was evaluated as 87.69 % and high binding affinity was established by the binding constant value, 1.16×10^7 M^{-1} using Langmuir binding isotherm plot. The estimated limit of detection (LOD) was 7.91×10^{-7} M which was lower than Environmental Protection Agency (EPA) recommendation. The probe also effectively responds to real sample analysis. The sensitivity and selectivity was realized due to the efficient FRET towards the fluorescence properties of $[Ru(bpy)_3]^{2+}$ complex.

Introduction

The worldwide use of pesticides pollute agricultural lands and impose toxic effects over the ecosystem.[1] The occurrence of pesticide residues in food items is a serious threat to food safety and it is necessary to develop new sensor systems to make sure the level of pesticides in food.[2] Organophosphates are one of the classes of herbicides/pesticides which are also used as chemical warfare agents.[3] Glyphosate (GP) is an important organophosphate extensively used as herbicide in agriculture.[4] The utilization of GP beyond the limit causes adverse effects to animals,[5] plants[4b] and results in the proliferation of breast cancer in humans.[6] The GP inhibits the aromatic amino acids synthesis by restricting the 5-enolpyruvylshikimate-3-phosphate synthase enzyme's activity which leads to plant's death.[7] The use of excess quantity of GP causes gene species shift and leads to genetically modified weeds.[8]

The widespread use of GP requires selective and sensitive detection. The Environmental Protection Agency (EPA) referred 2 mg/kg/day as a permissible dosage for GP.[9] The maximum contaminant level of GP in drinking water is reported as 0.7 ppm.[10] Quantitative determination of GP generally relies on solid-phase extraction followed by GC-MS[11] or LC-MS.[12] The enzyme-linked immunosorbent assay (ELISA) system is also used to determine GP.[13] Even though, these methods are reliable and accurate, they involve high cost and trained manpower. The various techniques proposed for sensing GP are fluorescent,[14] colorimetric detection,[15] electrochemical,[16] biosensor based on surface plasmon resonance[17] and quantum dot based sensor systems.[18] Optical recognition based on supramolecular interactions appears to be an appealing strategy.[19]

The fluorescence resonance energy transfer (FRET) based sensor systems receive predominant impact in selective detection of neutral and charged small molecules.[20] The utilization of FRET with solid state dye doped nanoparticles are novel strategies developed for selective detection, stability and reusability.[21] The cavity containing supramolecules are promising candidates for the selective recognition and sensitive detection.[22] In particular, the calixarenes are well-known vase structured supramolecules which are extensively employed in the field of molecular recognition.[23] Owing to their facile synthesis, flexibility, easy functionalization of upper and lower rims and tuning the cavity as per the requirements for particular analyte made calixarenes as most suitable among other host molecules.[24] Calixarene derivatives could be grafted over the luminescent nanoparticles for the optical detection of analytes.[25] Herein we report, *p*-tert-butylcalix[4]arene grafted ruthenium(II)-bipyridine doped silica nanoparticle for the FRET based selective detection of GP in aqueous medium.

Results and Discussion

Preparation and characterization of RSC

The RSC have been synthesized by multistep process (Figure 1).

[a] B. M. Ashwin, C. Saravanan, Dr. T. Stalin and Dr. P. Muthu Mareeswaran*
Department of Industrial Chemistry
Alagappa University
Karaikudi, Tamilnadu, India.
[b] Dr. S. Rajagopal*
Department of Physical Chemistry, School of Chemistry
Madurai Kamaraj University
Madurai, Tamilnadu, India.
E-mail: muthumareeswaran@gmail.com, mareeswaran@alagappauniversity.ac.in, rajagopalseenivasan@yahoo.com

Supporting information for this article is given via a link at the end of the document.((Please delete this text if not appropriate))

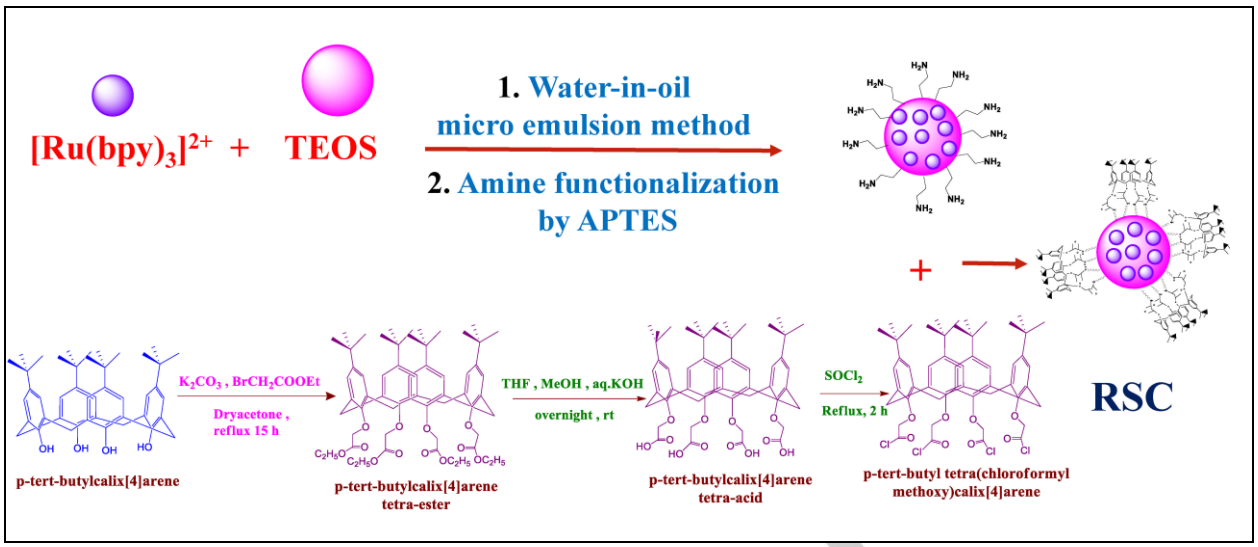

Figure 1. Multistep synthesis scheme for the $[Ru(bpy)_3]^{2+}$ dye doped silica nanoparticle coupled with *tert*-butylcalix[4]arene (RSC)

Each step is monitored by analytical techniques, the details are given in supporting information. A new peak at 450 nm of $[Ru(bpy)_3]^{2+}$ is observed in the UV-Visible absorption spectrum of Ru-SiNps which is not appeared in SiNps. The SEM images (Figure S3) of SiNps and Ru-SiNps explain the variation in the size of nanoparticles and the EDAX results establish the incorporation of $[Ru(bpy)_3]^{2+}$ within SiNps. The prepared *t*-butylcalix[4]arene tetra-ester and *t*-butylcalix[4]arene tetra-acid are characterized by FT-IR, ESI-MS, ^{1}H and ^{13}C NMR techniques and the results are given Figures S4 - S11. The mass peak of the corresponding product with Na^+ ion is appered at 1015.44 and 903.26 m/z in ESI-MS spectrum of *t*-butylcalix[4]arene tetra-ester (Figure S5) and *t*-butylcalix[4]arene tetra-acid (Figure S9), strongly confirmed the formation of these compounds. The final product, RSC is characterized by TEM, XRD and FT-IR.

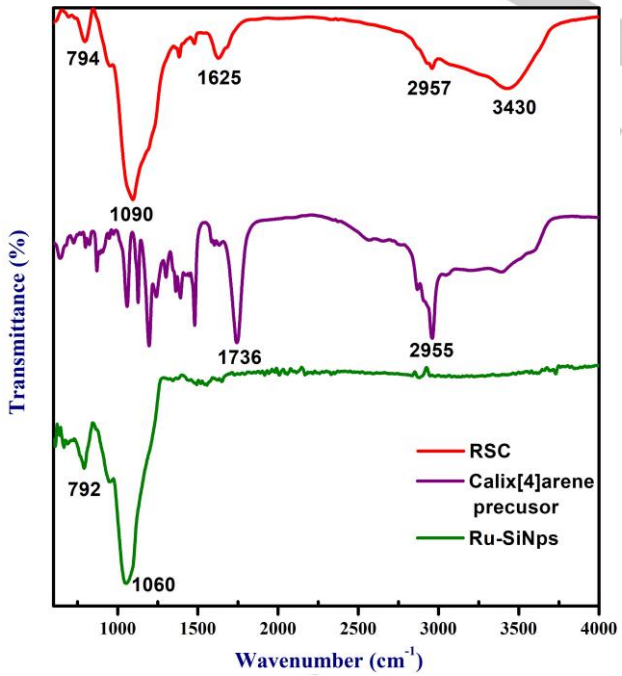

Figure 2. FT-IR spectra of the prepared RSC, calix[4]arene precursor and Ru-SiNps

The FT-IR spectra of RSC, Ru-SiNps and calix[4]arene precursor (Figure 2) confirm the successful grafting of the calix[4]arene on the surface of Ru-SiNps. From the IR spectra collected in Figure 2 we realize that RSC shows benzene ring stretching at 1625 cm^{-1}.[26] The sharp peak at 1090 cm^{-1} is the characteristic peak of Si–O–Si.[27] The C = O stretching band of the amide at 1736 cm^{-1} is significantly shifted and merged with the absorption band of benzene ring of RSC.[26] The absorption band at 794 cm^{-1} belongs to the C−H bending vibration of aromatic rings. This peak is present in both Ru-SiNps and RSC. It clearly confirms the presence of aromatic bipyridine moiety in solid matrix of RSC. The absorption band at 2957 cm^{-1} belongs to the C−H stretching vibration of alkanes in calix[4]arene conjugate. The broad peak at 3430 cm^{-1} is due to the N−H stretching frequency of amide formed in RSC. Hence, the FT-IR results confirm the formation of RSC.

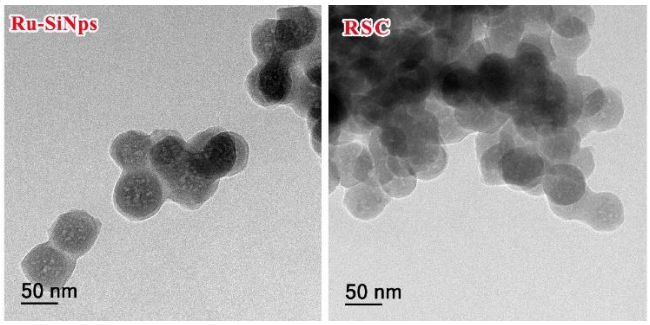

Figure 3. TEM images of Ru-SiNps and RSC

The XRD patterns of RSC and Ru-SiNps show the amorphous nature of the nanoparticles and distinct patterns (Figure S12). From TEM images (Figure 3), the remarkable differences in surface and size are observed. It can be seen that the prepared RSC is spherical in shape, highly dispersed and uniform in size (average size: 50 nm). The probe shows high stability with the environment.

FRET Based Selective Detection of GP

In order to examine the selectivity of FRET system towards GP, the FRET response of RSC with various common pesticides are carried out. GP only brings the FRET emission peak of $[Ru(bpy)_3]^{2+}$ dye at 580 nm and others fail to switch on the FRET emission. The emission intensity of GP-RSC combination at 580 nm is much higher than the others (Figure4). This is due to the significant interaction and proximity of GP with RSC. Since the number of GP molecules increases and FRET is rather strong, the emission intensity of GP (420 nm) also increases stepwise due to the availability of excess unbound GP and similar increment was observed in the recent report.[28] Moreover the probe is excited with the same wavelength of GP for another pesticide Mancozeb (340 nm), the FRET emission is not occurred at 580 nm. The competitive recognition is studied using the mixture of all pesticides with the probe. The interference of other pesticides in the recognition of GP is very meagre. This outcome strongly certifies the selective response of the probe. Thus a very simple calixarene functionalized luminescent nanomaterial RSC worked as a selective and sensitive FRET-On sensor for GP.

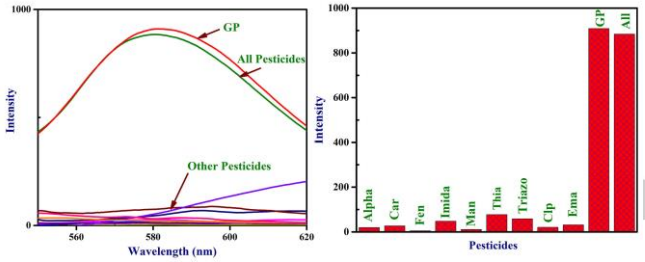

Figure 4. FRET response of RSC with individual common commercial pesticides including glyphosate (GP) and mixture of all pesticides. (Excited at individual excitation wavelengths of pesticides). The bar diagram shows the selective FRET-On response of GP.

Real Sample Analysis

To evaluate the practicality of RSC as a probe for GP, we carried out the real sample analysis by analyzing environmental ground water and rice samples.[29] Different concentrations of GP (1 and 2 μM) were added for each sample to determine recovery.The FRET spectrum of GP spiked real samples were measured (Figure 5) and the results were depicted in Table 1.

Table 1.FRET based detection of GP in real samples using RSC

Samples	pH	Added (μM)	Found (μM)	Recovery %
Ground water	6.6	1	0.963	96.3
		2	1.896	94.8
Rice	4.3	1	0.987	98.7
		2	1.955	97.7

The satisfactory recovery was observed in the range of 94–98% for different GP spiked water and grain samples, indicating the reported probe is good in precision. The pH of the real samples were measured and they show varient in pH. Interestingly all the samples give sufficient results using RSC, which supports the high stability and applicability of the probe in various conditions. These results confirm the applicability and reliability of the proposed method for assay of GP in environmental samples.The reported solid state probe has possibilities to be extended to the sensor strip like devices for direct detection of GP in real samples.[30]

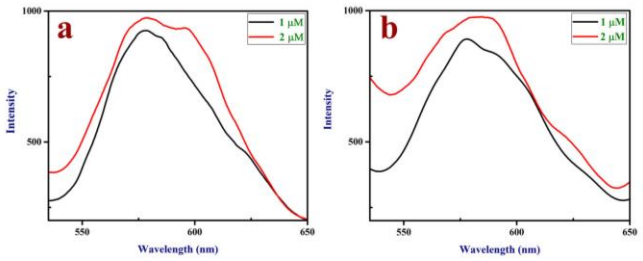

Figure 5. FRET emission spectrum of RSC with real samples (a) ground water and (b) rice spiked with different concentrations of GP.

Mechanism for the FRET response towards GP by RSC

The FRET response of RSC with GP is studied using fluorescence spectroscopy. The well-defined structure of the calixarene cavities can be exploited for the inclusion of organic guests.The calix[4]arene moiety grafted on silica matrix has a unique cavity with the size around 2.75-3.00 Å.[31] The size of GP is compatible with this size. However, the cavity of calix[4]arene is not sufficiently large enough to accommodate bulk aromatic pesticides excluding a small linear molecule like GP, which results in the selective FRET response to GP.[32] The hydrogen bond formation between the GP with the amide which is located at the lower rim of calix[4]arene is also responsible for the recognition. Similar recognition of amino acids with the calix[4]arene having amide group at the lower rim is reported previously.[33] This inclusion renders stable proximity with SiNps doped with $[Ru(bpy)_3]^{2+}$.There is a prominent overlap of the emission of GP with the absorption of $[Ru(bpy)_3]^{2+}$ (Figure S14), which facilitates the energy transfer between GP and $[Ru(bpy)_3]^{2+}$.The other pesticides taken for this study are not able to provide compact binding with RSC. Therefore, the possibility of FRET is less. The mechanism of FRET switch-on sensor with GP is explained in Figure 6.

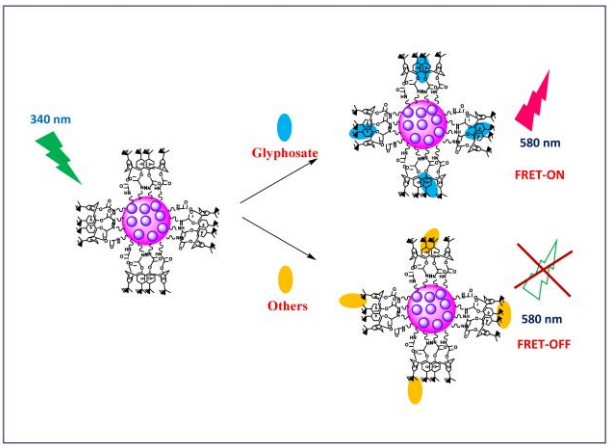

Figure6. Schematic representation of the FRET-On detection system for glyphosate (GP) using RSC

Binding and Detection Limit Studies of GP with RSC

The broad absorption peak of RSC overlaps that with GP, which makes the possibility of the binding constant calculation by absorption technique difficult. Moreover the reported sensor probe mainly works on the FRET principle. Hence the calculation of the binding constant by FRET emission change seems to be proper and suitable one. The concentration dependent change in emission intensity follows the binding of GP in the cavity of the receptor calix[4]arene grafted over the surface of RSC and the binding is effectively described by a Langmuir-type binding isotherm.[32, 34] The emission intensity is increased with increasing GP concentration (Figure7).

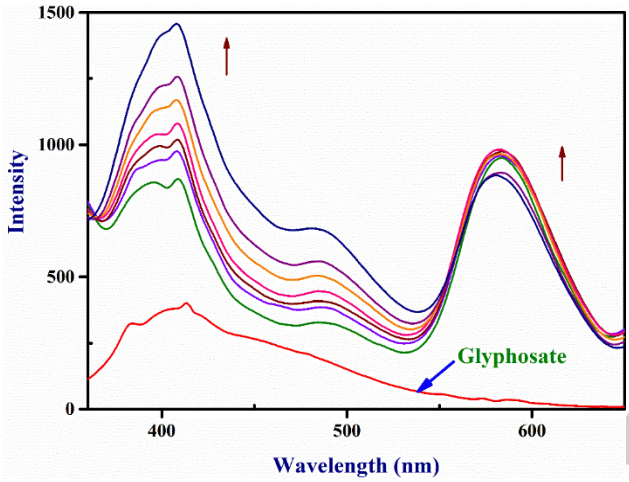

Figure7. FRET response of RSC with different concentrations of GP (0-2 µM). (Excited at 340 nm)

From the Langmuir equation, the surface of the RSC contains limited number of binding sites and each can adsorb single analyte (GP) from the solution. Θ is defined as the fraction of engaged sites. The binding rate of GP on the surface of RSC is proportional to the concentration of GP ([GP]) in the sample and the available binding sites, 1 - Θ. The binding rate (R_b) of GP on the surface of RSC is considered as,

$$R_b = K_b[GP](1 - \Theta) \quad (1)$$

The desorption rate of GP from the surface of RSC depends on the engaged binding sites fraction which is expressed as

$$R_b = K_d\Theta \quad (2)$$

At equilibrium, the binding rate is equal to the desorption rate

$$K_d\Theta = K_b[GP](1 - \Theta) \quad (3)$$

The solved equation for Θ is the function of the ratio, $B= K_b/K_d$.

$$\Theta = (B[GP])/(1 + B[GP]) \quad (4)$$

The ratio of the signal received at stated pesticide concentration I and the maximum intensity I_{max} is related to the fraction of the engaged binding sites, Θ.

$$\Theta = I/I_{max} \quad (5)$$

However, an equation relating the concentration of GP with the intensity of the signal can be derived as

$$I/I_{max} = (1/BI_{max}) + (1/I_{max})\,[GP] \quad (6)$$

It can be linearized as,

$$[GP]/I = (1/BI_{max}) + (1/I_{max})\,[GP] \quad (7)$$

As per the Langmuir description, a plot of [GP]/I as a function of [GP] should be linear when the binding of GP on the surface of RSC is factual. Here, [GP] is the GP's concentration and I is the fluorescence intensity of the RSC produced by FRET at given GP concentrations. Interestingly a linearity is obtained for the whole range of GP concentration. The binding constant, B is calculated as 1.16×10^7 M^{-1}, and the linear fit coefficient is > 0.999 (Figure 8). The remarkable Langmuirian fit suggests that, the binding probability is more than one for each GP to the surface of an individual Nps.

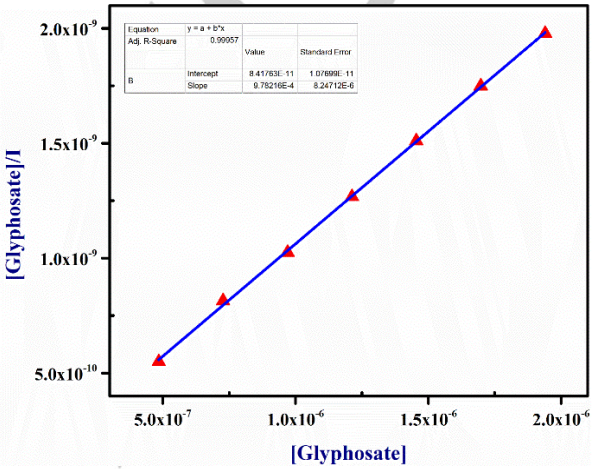

Figure8. Langmuir binding isotherm plot of GP with RSC showing a linear fit

The observed emission intensity changes of GP at the concentration 0 - 2 µM are correlated with the structural deformation of the calix[4]arene-group shell covering the Ru-SiNps upon intercalation. This may be due to the production of an effective and new radiative path involving the bound GP and/or from the nonradiative process suppression. Whenever GP is added with RSC, the intercalation of GP restricts the calixarene-cavity distortion and induces a static arrangement. Such uniformed orientation and/or conformational rigidity enhancement due to the surface substituents may restrict the quenching path to the medium by effective core protection and which increase the FRET intensity.

The change of FRET intensity can be described to the amount of GP bound to the sensing interface and the detection limit was calculated from the calibration plot (Figure S15).[35] A limit of detection about 7.91×10^{-7} M was found for GP, significantly lower than the maximum contaminant level allowed by EPA (0.7 ppm ≈4 µM).[19b]

FRET Efficiency Calculation

FRET is responsible for the appearance of acceptor's (RSC) emission while exciting the donor (GP) atom (Figure 4).[23a]

According to Förster's theory,[36] FRET efficiency (E) is given by,

$$E = (R_0^6)/(R_0^6+R^6) \quad (8)$$

where, R_0 is the Förster radius and R is the distance of acceptor center from the donor center. Förster radius is given by Eq.(9).

$$R_0 = (8.8 \times 10^{23} J K^2 Q_0 n^{-4}) 1/6A \quad (9)$$

$$J = \Sigma F(\lambda)\varepsilon(\lambda)\lambda^4\lambda / \Sigma F(\lambda)\lambda \quad (10)$$

Here, K^2 is the orientation factor of a dipole–dipole interaction, Q_0 is the quantum yield of donor in the absence of acceptor, J is the spectral overlap integral in $M^{-1}cm^3$ and n is the refractive index of the medium. Figure S14 in the supporting information shows the GP's emission overlap with the RSC's absorption. From the overlapping spectrum, J can be estimated by integrating the spectra from 360 nm to 550 nm. The estimated overlap integral value is 6.61×10^{-19} cm^3mol/L and the R_0 is 6.93 Å. For this calculation K^2 value is taken as 2/3 for random orientation, and n = 1.33 for water medium.

Interaction between GP and RSC probe system is associated with the existence of specific binding site on RSC. RSC has a supramolecular host molecule calix[4]arene as a binding site. The binding site and the cavity play important role in the specific interaction of RSC with GP. While binding of analyte occurs inside the cavity, the fluorophore donor will be very closer to the acceptor, RSC. The average distance is assumed from Ru-SiNps surface to the GP which is in the centre of the cavity and estimated as 5Å for the FRET efficiency, E is estimated as 87.69 % for GP-RSC system.

Conclusions

Luminescent silica nanoparticles grafted with *p*-tert-butylcalix[4]arene are synthesised and successfully applied to the detection of GP by means of FRET process using emission spectral technique. The FRET switch on process for RSC is observed in the presence of GP with 87.69% FRET efficiency and 7.91×10^{-7} M of detection limit. This FRET switch on is not observed for the pesticides other than GP taken for the study. The binding constant values establish the efficient binding of GP with cavity of *p*-tert-butylcalix[4]arene derivative grafted on the silica surface. The real time analysis depicts the efficiency of the RSC towards practical applications. The selective detection of GP using RSC by means of switch on FRET process shows the possible usage of FRET process in solid state sensor systems. The aspect of FRET based stable and simple sensor strips can be envisaged by means of this study.

Experimental Section

Materials

The $RuCl_3.3H_2O$, 2,2'-bipyridine, Triton X-100, *p*-tert-butylcalix[4]arene are procured from Sigma-Aldrich. (3-aminopropyl)triethoxysilane (APTES), tetraethyl orthosilicate (TEOS), ammonium hydroxide, ethanol, acetone,cyclohexane, 1-hexanol, potassium carbonate and ethyl bromoacetate are procured from Alfa Aesar. Ultra-pure water (Millipore) is used as solvent throughout the study. The pesticides Mancozeb (Man), Thiamethoxam (Thia), Cartap Hydrochloride (Car), Emamectin Benzoate (Ema), Alphamethrin (Alp), Fenpropathrin (Fen), Triazophos (Tri), Imidacloprid (Imi), Glyphosate (GP) and Chlorpyrifos (Chl) are purchased as commercial products SAAF, Pele, Quick, Trust, Alphaguard, Danitol, Tarzan, Pronto, Round Up and Durmet respectively. The chemical structure and absorption spectra (Figure S13& S2) of GP are given in Supporting Information.

Instruments

UV-Visible absorption spectrometric measurements and fluorescence emission measurements are performed by SHIMADZU UV-2401PC and JASCO FP-8200 Spectrofluorometer respectively at room temperature. FT-IR spectra are recorded on Jasco FT-IR 4600 spectrometer. The X-ray powder diffraction (XRD) is recorded on XPERT-PRO X-ray diffractometer with Cu-Kα radiation. Surface morphological studies and EDAX are carried out on FEI QUANTA 250 scanning electron microscope and TEM images are obtained by JEOL JEM 3010 Microscope.

Preparation of $[Ru(bpy)_3]^{2+}$ doped SiNps (Ru-SiNps)

Ru-SiNps were prepared by water-in-oil micro emulsion method.[37] Triton X-100 (1.77 ml), cyclohexane (7.5 ml), 1-hexanol (1.8 ml), water (400 µL) and concentrated solution of $[Ru(bpy)_3]^{2+}$(50 µL) were taken in a RB flask and stirred vigorously. After 1 h, TEOS (200 µL) as a precursor of silica was added to the solution and 100 µL of NH_4OH was added to initiate the polymerization process. The reaction was continued for 24 h at room temperature. The surface of the SiNps was modified by the addition APTES (100 µL) and TEOS (50 µL). The reaction mixture was stirred for further 2 h. The spherical shaped Ru-SiNps were separated by centrifugation. Then the Ru-SiNps were washed with water, ethanol and acetone several times. The bare SiNps were synthesized without $[Ru(bpy)_3]^{2+}$ and compared with Ru-SiNps using HR-SEM and EDAX (Figure S3).

Synthesis of *t*-butylcalix[4]arene precursor

The *t*-butylcalix[4]arene precursor was synthesized according to the reported procedure[26] with some modifications. A mixture of *p*-*tert*-butylcalix[4]arene (1g), potassium carbonate (0.42 g) and ethylbromoacetate (0.68 ml) were taken in 50 ml dry acetone and refluxed for 15 h. The cooled solution was passed through a bed of celite. The filtrate and dichloromethane washings of celite were mixed and evaporated to dryness. Recrystallization from ethanol provided the tetra-ester. A solution of prepared tetra-ester (98 mg) in a mixture of THF (3 mL), methanol (3 mL) and aqueous KOH (1 mL, 40% weight) was stirred overnight at room temperature. The organic solvents were removed *in vacuo*at 70 ºC and the remaining aqueous solution was acidified to pH 1 by the addition of 4 N HCl and allowed to stand at 0 ºC for 6 h. The resulting precipitate was filtered, washed with water and dried at 80 ºC. The tetra-acid was extracted from aqueous solution with CH_2Cl_2. The resulting white solids were dried under vacuum. The product was characterized using FT-IR and discussed in the results and discussion part.

Preparation of *t*-butylcalix[4]arene grafted Ru-SiNps(RSC)

The prepared t-butylcalix[4]arene tetra-acid (1.76 g) was then refluxed with 20 ml of thionyl chloride for 2 h to obtain *p*-tert-butyl-tetra(chloroformylmethoxy)calix[4]arene in quantitative yield, and the excessive thionyl chloride was removed in vacuum. The obtained product was directly used in next step without further purification. A mixture of calix[4]arene precursor (0 .76 g), Ru-SiNps (0.94 g, content ~90%) and triethylamine (0.33 g) in freshly distilled dry toluene (120 ml) were stirred at room temperature in an inert atmosphere of dry nitrogen for 16 h. At last, the solid product was filtered and washed in sequence with warm toluene, acetone, methanol and double-distilled water subsequently. The product was dried under vacuum for 3 h, and kept in a desiccator.The normalised UV and emission spectra of RSC in water are shown in Figure S1.

FRET Studies

The chemical composition of the desired pesticide in the commercial pesticides were calculated. Each pesticide (1×10^{-6} M) was

taken with RSC (1 mg) in 5 ml SMF separately. Each samples were sonicated and emission spectra was measured using fluorescence spectrometer by exciting at the excitation wavelength of corresponding pesticide. For GP titration study, 1 mg of RSC was taken in a cuvette and GP was varied from 0 - 2 µM concentration. The whole study was carried out in double distilled ultrapure water (pH=6.8) and room temperature.

Real Sample Analysis

To find the potential applicability of the proposed RSA in real samples, detection of GP residues was carried out in ground water and rice grains. From the literature, these are the suitable samples for pesticide detection in real samples.[29b] The collected ground water sample was filtered using filter paper to remove solid particulates from the samples. Then the water samples were spiked with different concentrations of GP (1×10^{-4} M and 2×10^{-4} M) and analyzed by RSC. The spiked rice sample was prepared according to a previous report.[29a] Similarly, different concentrations of GP (1×10^{-4} M and 2×10^{-4} M) were added into the fine powdered rice samples (10.0 g) and kept for 24 h at room temperature. Then, GP was extracted using 20 mL of methanol in an ultrasonic bath for 20 min. The extracts were decanted and repeated the same procedure twice. The extract was filtrated through filter paper and then the concentration of GP was estimated using RSC as a probe.

Acknowledgements

The authors acknowledge the financial support of Department of Science and Technology (DST INSPIRE) [Project number – IFA14/CH-147], India. B. M. Ashwin thanks to Alagappa University for providing AURF Fellowship for his research work.

Keywords : FRET-On Sensor• Glyphosate• Pesticide Detection• Calixarene• Luminescent Nanoparticle

[1] X. Zeng, J. Ma, L. Luo, L. Yang, X. Cao, D. Tian, H. Li, *Org. Lett.* **2015**, *17*, 2976-2979.

[2] a) F. Zhang, Y. Sun, D. Tian, W. S. Shin, J. S. Kim, H. Li, *Chem. Commun.* **2016**, *52*, 12685-12693; b) T. Wang, R. C. Reid, S. D. Minteer, *Electroanal.* **2016**, *28*, 854-859.

[3] M. J. Tan, Z.-Y. Hong, M.-H. Chang, C.-C. Liu, H.-F. Cheng, X. J. Loh, C.-H. Chen, C.-D. Liao, K. V. Kong, *Biosens. Bioelectron.* **2017**, *96*, 167-172.

[4] a) K. Mahendrakar, P. M. Venkategowda, S. M. Rao, D. P. Mutkule, *Indian J. Crit. Care Med.* **2014**, *18*, 328-330; b) J. M. Green, *Pest Manag. Sci.* **2014**, *70*, 1351-1357.

[5] a) P. I. Ingaramo, J. Varayoud, M. M. Milesi, M. Guerrero Schimpf, R. Alarcón, M. Muñoz-de-Toro, E. H. Luque, *Reproductive Toxicol.* **2017**, *73*, 87-95; b) C. M. Howe, M. Berrill, B. D. Pauli, C. C. Helbing, K. Werry, N. Veldhoen, *Environ. Toxicol. Chem.* **2004**, *23*, 1928-1938.

[6] S. Thongprakaisang, A. Thiantanawat, N. Rangkadilok, T. Suriyo, J. Satayavivad, *Food Chem. Toxicol.* **2013**, *59*, 129-136.

[7] H. C. Steinrücken, N. Amrhein, *Biochem. Biophys. Res. Commun.* **1980**, *94*, 1207-1212.

[8] J. M. Green, M. D. K. Owen, *J. Agric. Food Chem.* **2011**, *59*, 5819-5829.

[9] J. F. Acquavella, B. H. Alexander, J. S. Mandel, C. Gustin, B. Baker, P. Chapman, M. Bleeke, *Environ. Health Perspect.* **2004**, *112*, 321-326.

[10] T. Minami, Y. Liu, A. Akdeniz, P. Koutnik, N. A. Esipenko, R. Nishiyabu, Y. Kubo, P. Anzenbacher, *J. Am. Chem. Soc.* **2014**, *136*, 11396-11401.

[11] T. Saito, H. Aoki, A. Namera, H. Oikawa, S. Miyazaki, A. Nakamoto, S. Inokuchi, *Anal. Sci.* **2011**, *27*, 999-999.

[12] a) H. A. Martins-Junior, D. T. Lebre, A. Y. Wang, M. A. Pires, O. V. Bustillos, *Rapid Commun. Mass Spectrom.* **2009**, *23*, 1029-1034; b) A. Ghanem, P. Bados, L. Kerhoas, J. Dubroca, J. Einhorn, *Anal. Chem.* **2007**, *79*, 3794-3801.

[13] J. Sanchís, L. Kantiani, M. Llorca, F. Rubio, A. Ginebreda, J. Fraile, T. Garrido, M. Farré, *Anal. Bioanal. Chem.* **2012**, *402*, 2335-2345.

[14] a) W. Xuan, Y. Cao, J. Zhou, W. Wang, *Chem. Commun.* **2013**, *49*, 10474-10476; b) T. J. Dale, J. Rebek, *J. Am. Chem. Soc.* **2006**, *128*, 4500-4501; c) Y. Hu, L. Chen, H. Jung, Y. Zeng, S. Lee, K. M. K. Swamy, X. Zhou, M. H. Kim, J. Yoon, *ACS Appl. Mater. Interfaces* **2016**, *8*, 22246-22252.

[15] a) A. Balamurugan, H.-i. Lee, *Macromolecules* **2016**, *49*, 2568-2574; b) J. Zheng, H. Zhang, J. Qu, Q. Zhu, X. Chen, *Anal. Methods* **2013**, *5*, 917-924.

[16] a) E. A. Songa, O. A. Arotiba, J. H. O. Owino, N. Jahed, P. G. L. Baker, E. I. Iwuoha, *Bioelectrochemistry* **2009**, *75*, 117-123; b) B. S. Clegg, G. R. Stephenson, J. C. Hall, *J. Agric. Food Chem.* **1999**, *47*, 5031-5037.

[17] X. Ding, K.-L. Yang, *Anal. Chem.* **2013**, *85*, 5727-5733.

[18] D. Wang, B. Lin, Y. Cao, M. Guo, Y. Yu, *J. Agric. Food Chem.* **2016**, *64*, 6042-6050.

[19] a) Y. Liu, M. Bonizzoni, *J. Am. Chem. Soc.* **2014**, *136*, 14223-14229; b) M. Wang, H. Ye, L. You, X. Chen, *ACS Appl. Mater. Interfaces* **2016**, *8*, 574-581.

[20] a) X. Wu, Y. Song, X. Yan, C. Zhu, Y. Ma, D. Du, Y. Lin, *Biosens. Bioelectron.* **2017**, *94*, 292-297; b) F. Du, Y. Min, F. Zeng, C. Yu, S. Wu, *Small* **2014**, *10*, 964-972.

[21] E. Babu, P. M. Mareeswaran, S. Rajagopal, *J. Fluoresc.* **2013**, *23*, 137-146.

[22] a) X. Zhou, S. Han, Q. Zhang, Y. Dou, J. Guo, L. Che, X. Li, J. Zhang, *Polym. Chem.* **2015**, *6*, 3716-3727; b) B. M. Ashwin, A. Herculin Arun Baby, M. Prakash, M. Hochlaf, P. Muthu Mareeswaran, *J. Phys. Org. Chem.* **2018**, *31*, e3788.

[23] a) P. M. Mareeswaran, D. Maheshwaran, E. Babu, S. Rajagopal, *J. Fluoresc.* **2012**, *22*, 1345-1356; b) G. Nie, Y. Sun, F. Zhang, M. Song, D. Tian, L. Jiang, H. Li, *Chem. Sci.* **2015**, *6*, 5859-5865; c) B. M. Ashwin, A. Vinothini, T. Stalin, P. Muthu Mareeswaran, *ChemistrySelect* **2017**, *2*, 931-936.

[24] a) T. Hanauer, R. J. Hopkinson, K. Patel, Y. Li, D. Correddu, A. Kawamura, V. Sarojini, I. K. H. Leung, T. Gruber, *Org. Biomol. Chem.* **2017**, *15*, 1100-1105; b) X. Chi, G. M. Peters, F. Hammel, C. Brockman, J. L. Sessler, *J. Am. Chem. Soc.* **2017**, *139*, 9124-9127; c) B. M. Ashwin, C. Saravanan, M. Senthilkumaran, R. Sumathi, P. Suresh, P. Muthu Mareeswaran, *Supramol. Chem.* **2018**, *30*, 32-41.

[25] a) F. Zou, B. Wu, X. Wang, Y. Chen, K. Koh, K. Wang, H. Chen, *Sensors Actuat. B: Chem* **2017**, *241*, 160-167; b) P. G. Sutariya, A. Pandya, A. Lodha, S. K. Menon, *Talanta* **2016**, *147*, 590-597.

[26] X.-Z. Xiao, Y.-Q. Feng, S.-L. Da, Y. Zhang, *Anal. Lett.* **2000**, *33*, 3355-3372.

[27] T. Li, Y. Zhou, J. Sun, D. Tang, S. Guo, X. Ding, *Microchim. Acta* **2011**, *175*, 113.

[28] L. Olejko, I. Bald, *RSC Adv.* **2017**, *7*, 23924-23934.

[29] a) J. V. Rohit, R. K. Singhal, S. K. Kailasa, *Sensors Actuat. B: Chem* **2016**, *237*, 1044-1055; b) N. Fahimi-Kashani, M. R. Hormozi-Nezhad, *Anal. Chem.* **2016**, *88*, 8099-8106.

[30] a) X. Huang, Z. P. Aguilar, H. Li, W. Lai, H. Wei, H. Xu, Y. Xiong, *Anal. Chem.* **2013**, *85*, 5120-5128; b) C.-C. Fang, C.-C. Chou, Y.-Q. Yang, T. Wei-Kai, Y.-T. Wang, Y.-H. Chan, *Anal. Chem.* **2018**, *90*, 2134-2140.

[31] S. J. Dalgarno, J. L. Atwood, C. L. Raston, *Cryst. Growth Des.* **2006**, *6*, 174-180.

[32] H. Li, F. Qu, *Chem. Mater.* **2007**, *19*, 4148-4154.

[33] a) A. Acharya, B. Ramanujam, J. P. Chinta, C. P. Rao, *J. Phys. Chem.* **2011**, *76*, 127-137; b) M. Tabakci, B. Tabakci, M. Yilmaz, *J. Incl. Phenom. Macrocycl. Chem.* **2005**, *53*, 51-56; c) P. Muthu Mareeswaran, E. Babu, S. Rajagopal, *J. Fluoresc.* **2013**, *23*, 997-1006.

[34] T. Li, Y. Zhou, J. Sun, K. Wu, *Am. J. Analyt. Chem.* **2012**, *3*, 7.

[35] B. M. Ashwin, G. Sivaraman, T. Stalin, R. Yuvakkumar, P. M. Mareeswaran, *J. Photochem. Photobiol. B* **2018**, *183*, 302–308.

[36] G. Xue, Z. Yue, Z. Bing, T. Yiwei, L. Xiuying, L. Jianrong, *Analyst* **2016**, *141*, 4941-4946.

[37] H. Wei, J. Liu, L. Zhou, J. Li, X. Jiang, J. Kang, X. Yang, S. Dong, E. Wang, *Chem. Eur. J.* **2008**, *14*, 3687-3693.

10.1002/cphc.201800447

Layout 2:

ARTICLE

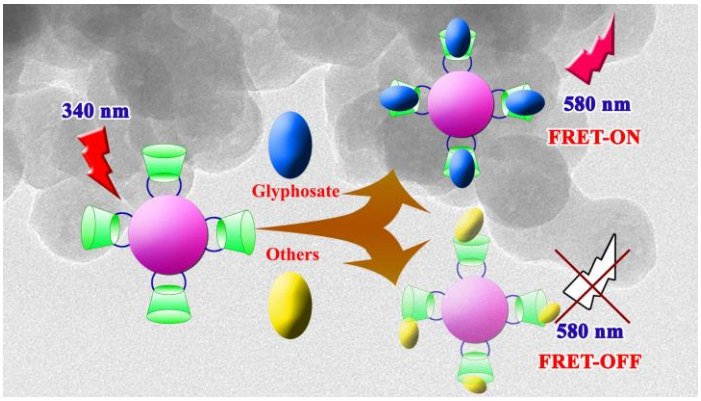

B. M. Ashwin, C. Saravanan, Dr.T. Stalin, Dr. P. Muthu Mareeswaran and Dr. S. Rajagopal**

1 – 7

FRET based solid state luminescent sensor for glyphosate using calixarene grafted ruthenium(II) bipyridine doped silica nanoparticle

A calixarene functionalized luminescent silica nanoparticle was prepared and studied for it's FRET based selective and sensitive sensor application for glyphosate.